ON THE USE OF OBSERVABILITY MEASURES FOR SENSOR LOCATION IN TUBULAR REACTORS

Walter Waldraff and Denis Dochain
Cesame, Université Catholique de Louvain, av. G. Lemaître 4-6, 1348 Louvain-La-Neuve, Belgium
Fax: +32-10-472180, e-mail: dochain@auto.ucl.ac.be

Abstract In this paper we discuss the choice of sensor positions for a tubular reactor with a preset number of sensors. Different observability measures, based on the observability matrix, the observability gramian and the Popov-Belevitch-Hautus rank test are considered. The analysis is carried out on the reduced finite-dimensional model of the process. The results are put in perspective with the modal observability properties of the original infinite-dimensional model.

Keywords : tubular reactor, observability, sensor location, distributed parameter systems

1 Introduction

A common problem for monitoring and control of (bio)chemical processes is the general lack of sensors. In order to overcome this difficulty, model-based state estimation techniques (e.g. Kalman or Luenberger observers) can be used to estimate unmeasured variables. However, for a successful implementation, it has to be verified that the considered sensors are sufficient, i.e. that the process is observable. For distributed parameter systems (DPS), observability is not only affected by the choice of sensors but also by the sensor location. Beside the problem of designing efficient state observers based on the few available data, we are facing the problem of locating sensors at appropriate positions in order to obtain the best information about the process dynamics along the reactor (see also [8]). In this paper we discuss the choice of optimal sensor positions for a tubular reactor example with a preset number of sensors. The analysis is carried out on the infinite-dimensional and the reduced finite-dimensional models of the process. For the latter, different observability measures, based on the observability matrix [3, 9], the observability gramian [3] and the Popov-Belevitch-Hautus rank test [9] are considered.

2 Tubular reactor example

Let us consider a tubular reactor in which the first order reaction $A \longrightarrow b\,B$ takes place. In presence of axial dispersion, the process can be described by the following mass balance dynamical equations:

$$\frac{\partial x_1}{\partial t} = D_a \frac{\partial^2 x_1}{\partial z^2} - u\frac{\partial x_1}{\partial z} - k_0 x_1 \tag{1}$$

$$\frac{\partial x_2}{\partial t} = D_a \frac{\partial^2 x_2}{\partial z^2} - u\frac{\partial x_2}{\partial z} + b k_0 x_1 \tag{2}$$

where $x_1(z,t)$, $x_2(z,t)$, z, t, u, D_a and k_0 are the concentration of A and B, the axial space and time coordinates, the fluid superficial velocity (m/s), the axial dispersion coefficient (m^2/s), and the kinetic constant (s^{-1}), respectively. Let us also consider the Danckwerts boundary conditions :

$$D_a \frac{\partial x_1}{\partial z}(0,t) - u x_1(0,t) = -u x_{in}(t) \tag{3}$$

$$D_a \frac{\partial x_2}{\partial z}(0,t) - u x_2(0,t) = 0 \tag{4}$$

$$D_a \frac{\partial x_i}{\partial z}(l,t) = 0,\ i = 1,2 \tag{5}$$

Our observability analysis will be based on the assumption that only the concentration of B is measured at a selected sensor position z_s, i. e.:

$$y(t) = x_2(z_s,t) \tag{6}$$

The basic motivation of this choice is to have the lowest possible number of sensors. With that regard, A is not a good choice while B is : rigourous (see [5] and Section 3) (but also intuitive) observability analysis shows that the system is not observable from x_1 only, while it is from x_2. In sections 4 and 5, the analysis is based on a finite-dimensional approximation of the DPS

(1)-(6). In line with many works in process control (e.g. [7]), we have here considered orthogonal collocation where the state variables $x_1(z,t)$ and $x_2(z,t)$ are approximated by the following expansion $x_j(z,t) \approx \sum_{i=1}^{n_c} L_i(z) x_{j,i}^c(t)$, j = 1, 2. Herein, $x_{j,i}^c(t)$ is the value of $x_j(z,t)$ (j = 1, 2) at the collocation points $\underline{z}^c = [z_1^c, \ldots, z_{n_c}^c]^T$ for which $0 = z_1^c < z_1^c < \ldots < z_{n_c}^c = l$ holds. $L_i(z)$ are usually the Lagrange polynomials. Using this approximation the infinite-dimensional model given above is transformed into the finite-dimensional linear time-invariant model :

$$\dot{\underline{x}}_c = A\underline{x}_c + B\underline{u}, \qquad \underline{y} = C\underline{x}_c \tag{7}$$

Herein $\underline{x}_c(t) = [x_{1,2}^c(t), \ldots, x_{1,n_c-1}^c(t), x_{2,2}^c(t), \ldots, x_{2,n_c-1}^c(t)]$, and $\underline{u}(t) = x_{1,in}(t)$. To derive the system matrix A, the approximation of the states at the boundaries $\{0, l\}$ are expressed through (3)-(5) as a function of $\underline{x}_c(t)$ and $u(t)$.

3 Observability of the infinite dimensional linear model

Here we consider the modal observability because it is closely related to the approximate observability [4] and yet not too complex to evaluate. The analysis is based on the modal expansion of the system solution :

$$\begin{aligned}\underline{x}(z,t) &= \int_{\zeta=0}^{l} \underline{\underline{g}}(z,\zeta,t)\underline{x}_0(\zeta)\, d\zeta \\ &- \int_{\tau=0}^{t} \underline{\underline{g}}(z,0,t-\tau) \begin{bmatrix} -ux_{1,in}(\tau) \\ 0 \end{bmatrix} d\tau\end{aligned}$$

where $\underline{\underline{g}}(z,\zeta,t)$ is the Green's matrix function [4]. It can be obtained after some calculations by using the Laplace transform and the eigenfunction expansion, and is here equal to [11] :

$$\underline{\underline{g}}(z,\zeta,t) = \sum_{k=1}^{\infty} \phi_k(z)\psi_k(\zeta) \begin{bmatrix} a_{1k} & 0 \\ ba_{21k} & a_{2k} \end{bmatrix} \tag{8}$$

$$\begin{aligned}a_{ik} &= e^{\lambda_{i,k}t},\ i = 1,2;\ a_{21k} = a_{2k} - a_{1k} \\ \phi_k(z) &= e^{\frac{u}{2D_a}z} B_k\left(\tfrac{2D_a\omega_k}{u}\cos(\omega_k z) + \sin(\omega_k z)\right) \\ \psi_k(\zeta) &= e^{-\frac{u}{2D_a}\zeta} B_k\left(\tfrac{2D_a\omega_k}{u}\cos(\omega_k \zeta) + \sin(\omega_k \zeta)\right) \\ B_k &= [\left(\tfrac{2D_a\omega_k}{u}\right)^2\left(\tfrac{l}{2} + \tfrac{\sin(2\omega_k l)}{4\omega_k}\right) \\ &+ \tfrac{l}{2} - \tfrac{\sin(2\omega_k l)}{4\omega_k} + \tfrac{2D_a \sin^2(2\omega_k l)}{u}]^{-1/2} \\ \lambda_{2,k} &= -D_a\left(\left(\tfrac{u}{2D_a}\right)^2 + \omega_k^2\right),\ \lambda_{1,k} = \lambda_{2,k} - k_0\end{aligned}$$

Herein $\phi_k(z)$ and $\psi_k(\zeta)$ are the scalar dependencies of the eigenspace $V_k(z)$ and the adjoint eigenspace $\tilde{V}_k(\zeta)$, respectively. $\lambda_{1,k}$ and $\lambda_{2,k}$ are the eigenvalues associated to the equations (1) and (2), respectively. The eigenfrequencies ω_k are the solutions of the following expression :

$$2\omega_k\cos(\omega_k l) + \left(\frac{u}{2D_a} - \frac{2D_a\omega_k^2}{u}\right)\sin(\omega_k l) = 0 \tag{9}$$

By applying the eigenfunction expansion $\underline{X}(z,s) = \sum_{k=1}^{\infty} V_k(z)\underline{X}_k^*(s)$ to the output equation (6), it can be written as follows [11] :

$$\begin{aligned}Y(s) &= \underline{c}^T\underline{X}^* &(10)\\ \underline{c}^T &= [\phi_1(z_s)[-b/(\sqrt{1+b^2}) \quad 1] \\ &\quad \phi_2(z_s)[-b/(\sqrt{1+b^2}) \quad 1] \quad \ldots] &(11)\end{aligned}$$

with $\underline{X}^*$ the complete infinite-dimensional state vector (i.e. the system modes). Modal observability basically means that each mode is observable. In other words, the system will be modal observable if the sensor is placed at positions z_s where $\phi_k(z_s) \neq 0 \quad \forall\ k = 1, 2, \ldots$ The zeros $z_{z,i}$ are defined from (9) as follows :

$$z_{z,i} = \frac{\arctan(-\frac{2D_a\omega_k}{u})}{\omega_k} \tag{12}$$

These are plotted in Figure 1 for k= 1 to 10: we get a dense spectrum of zeros with increasing k in the interval $[0, l]$ (Note that there is no zero for k = 1). However, observability is guaranteed at z_s = 0 and $z_s = l$. Indeed, as $\omega_k \neq 0\ \forall\ k$ we have $\phi_k(0) = \frac{2D_aB_k\omega_k}{u} \neq 0\ \forall\ k$, and observability for $z_s = 0$ follows. From (8), (9), we have modal observability at $z_s = l$ if the conditions $l\omega_k \neq m\pi$ for $m = 0, \pm1, \pm2, \ldots$ and $\omega_k \neq \pm j\frac{u}{2D_a}$ for k = 1, 2,... are satisfied, which holds by definition of ω_k. The modal observability analysis allows us to conclude that the axial dispersion model is modal observable if the concentration of the product B is measured at the reactor output or at the reactor input, and that it is not modal observable if the sensor for B is positioned at locations corresponding to zeros of the model eigenfunctions.

Remark : if we consider the reactant A as the measured output, the system is not modal observable, since we don't have access to the modes of the product B (see the expression of $\underline{\underline{g}}(z,\zeta,t)$).

4 Observability of the finite dimensional model

As it is usually quite difficult to test the observability for a DPS, we consider the observability of the finite-dimensional approximation model (7), via 3 different observability measures.

4.1 Observability matrix based measure

A first interesting measure is based on the singular values of the observability matrix [9] $O_1 = [C^T, A^TC^T, (A^T)^2C^T, \ldots, (A^T)^{n-1}C^T]$ and can be written as follows:

$$\sigma_{min}(O_1) > 0 \tag{13}$$

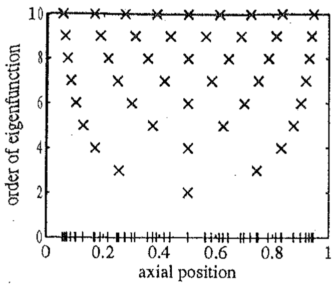

Figure 1: Eigenfunction zeros

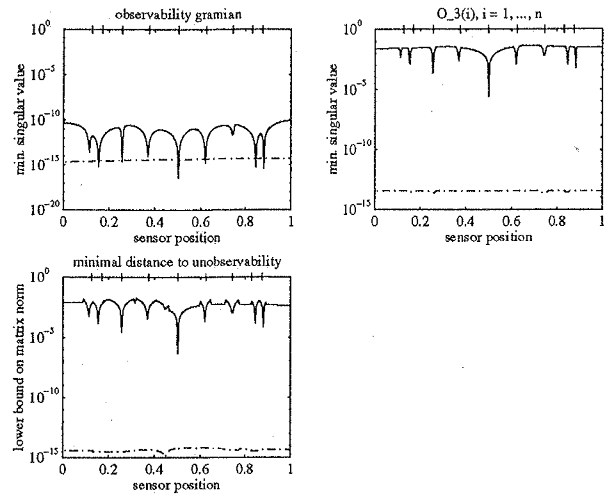

Figure 2: Observability measures

where $\sigma_{min}(O_1)$ is the minimal singular value of the observability matrix O_1. For numerical evaluation, we have also to consider the computational error in a singular value $\Delta\sigma(M)$ due to the finite word length representation. An estimation of the error upper bound is given by [1] through $|\Delta\sigma(M)| < p(r,c)\sigma_{max}(M)\epsilon$ where M is a $(r \times c)$-matrix, $p(r,c)$ is a slowly growing function of r and c, and ϵ is the relative accuracy of the used computer. In [10] the realization $p(r,c) = \min(r,c)$ is proposed. Including these restrictions into (13), we obtain an observability condition for the "worst case": $\sigma_{min}(O_1) - \min(r,c)\sigma_{max}(O_1)\epsilon > 0$. This can also be stated as follows by considering a modified condition number $\kappa_m(O_1)$:

$$\kappa_m(O_1) = \frac{\sigma_{min}(O_1)}{\sigma_{max}(O_1)} - nm\epsilon > 0 \qquad (14)$$

4.2 Observability gramian based measure

One drawback of the above conditions is their sensitivity to the state dimension : the observability matrix O_1 tends to be badly conditioned with the growing dimension of the state vector [3] :

$$\left|\frac{\lambda_{min}(A^{n-1})}{\lambda_{max}(A^{n-1})}\right| = \left|\frac{\lambda_{min}(A)}{\lambda_{max}(A)}\right|^{n-1} \qquad (15)$$

Thus, the minimal singular value $\sigma_{min}(O_1)$ may not be calculated with a sufficient precision for a valid observability measure. An alternative is to look at the observability gramian [3] :

$$G_o = \int_0^\infty e^{A^T t} C^T C e^{At}\, dt \qquad (16)$$

The observability test is then : $\text{rank}\{G_o\} = n$. So instead of O_1 the observability gramian G_o can also be used in conjunction with (13) (14).

4.3 Popov-Belevitch-Hautus rank test

Another test for observability which is also numerically interesting is the Popov-Belevitch-Hautus (PHB) rank test [9] : a pair (A, C) is observable if and only if

$$\text{rank}\begin{bmatrix} sI - A \\ C \end{bmatrix} = \text{rank}\,[O_2(s)] = n, \ \forall s \in \mathcal{C} (17)$$

Since for all s that are not eigenvalues of A, condition (17) is fullfilled (because then $\det(sI - A) \neq 0$ holds), the test reduces to :

$$\text{rank}\begin{bmatrix} \lambda_i I - A \\ C \end{bmatrix} = \text{rank}\,[O_3(\lambda_i)] = n \qquad (18)$$

$\forall \lambda_i, i = 1\ to\ n$ where λ_i is the i^{th} eigenvalue of A. An equivalent form for computational evaluation of (18), using singular values, is :

$$\bar{\sigma}_{min} = \min_{\lambda_i, i=1,\ldots,n} \{\sigma_{min}(O_3(\lambda_i))\} > 0, \qquad (19)$$

In [6] the following observability measure is given which uses the PBH rank test (17). Suppose E is the smallest perturbation (defined as that perturbation, which has the minimal 2-norm $||E||_2$) to the matrix A, that is needed to make the pair $(A+E, C)$ rank-deficient, i.e. unobservable. Then $||E||_2$, the minimal distance to the set of all unobservable pairs $(A + E, C)$, is given by the solution of the minimization problem :

$$||E||_2 = \min_{s \in \mathcal{C}} \sigma_{min} \begin{bmatrix} sI - A \\ C \end{bmatrix} \qquad (20)$$

However, since (20) is in general a nonconvex minimization problem, it is not an easy task to get $||E||_2$. As an alternative we propose to use the algorithm presented in [2] to calculate upper and lower bounds on $||E||_2$, and therefore to consider the lower bound as an observability measure.

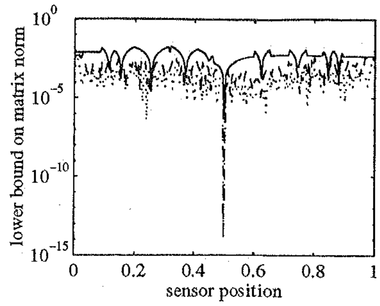

Figure 3: Minimal distance to unobservability $\|E\|_2$ ($n_c = 7$(-), 22(- -), 42(...))

4.4 Implementation

The different observability measures have been calculated for a sensor position z_s varying between 0 and l. The results presented in Figure 2 have been obtained for the following set of model parameters: $l = b = k_0 = 1$ and $u = D_a = 0.1$. The orthogonal collocation parameters have been chosen on the basis of model dynamics simulation. 7 collocation points (including the boundaries) chosen as the zeros of a Jacobi polynomial with its parameters $(\alpha, \beta) = (0, 0)$ were sufficient to obtain a good approximation. The minimal singular value of the observability gramian $\sigma_{min}(G_0)$ (16), the minimal singular value of $\{O_3(\lambda_i),\ i = 1, \ldots, n\}$ (18), and the lower bound on $\|E\|_2$ for a varying sensor position $0 \leq z_s \leq l$ are represented by straight lines in Figure 2 a, b and c, respectively. An estimate for the precision of these observability measures is given on each figure in dashed-dotted lines. In these plots we have also included the positions of the eigenfunction zeros (12) for $k = 1, \ldots, 5$, calculated in section 3, indicated by short vertical lines on the upper horizontal axis.

In Figure 2, the minimal singular value calculated from the observability gramian is by magnitudes smaller than the others. At some points its value becomes smaller than the numerical precision. This would lead to the conclusion that on the basis of the numerical computation precision, the process is unobservable at these points and observable for the rest of $[0, l]$. For the other observability measures, it can be concluded that the process is observable for all sensor positions $0 \leq z_s \leq l$. Note however that all the considered observability measures exhibit a peakwise decrease near the zeros of the low order eigenfunctions. This indicates that the collocation method represents an approximation for the low order eigenmodes of the distributed parameter model.

In Figure 3 the lower bound on the minimal distance to unobservability is shown for different numbers of collocation points (7, 22, 42). From this figure it can be concluded, that with a higher number of collocation points the observability measure becomes smaller for interior points, but remains almost constant at the boundaries $\{0, l\}$. Furthermore, the number of peaks increases : this indicates that with an increasing number of collocation points, more and more eigenvalues become important in the approximation, and the observability measure tends to the result which was obtained for the infinite-dimensional model.

At this point we can conclude that when the computation of the system eigenmodes is too complex, the orthogonal collocation appears to be an interesting approximation for the (modal) observability analysis because of its ability to fairly approximate the loss of observability at the zeros of the dominant system eigenfunctions. Note also that the low order eigenmodes are dominant because their corresponding eigenvalues are proportional to ω_k^2 which are increasing in k.

5 Sensor positioning

Up to now, the results that we have obtained in Section 3 are not very useful to know what should be the best locations for the sensor, except that maybe the output and the input of the reactor seem to be the best ones. We shall now treat the question : what is the best choice of a sensor position for a given discretized model, with possibly some uncertainty in the model parameters?

Any of the observability measures introduced in Section 4, could be used to define a criterion for sensor positioning. All of these criterias use the minimal singular value of a matrix, say M_0. If we also consider the numerical value computation precision, the optimization of the sensor location consists of maximizing :

$$I = \sigma_{min}(M_0) - \min(r, c)\sigma_{max}(M_0)\epsilon \qquad (21)$$

applied to the $(r \times c)$-observability matrix M_0. Among the different matrices considered in section 4, O_2 (related to the PBH test) has the advantage that the value of the maximized criterion (21) can be interpreted as the allowable pertubation to the system matrix A. But if O_2 is applied to (21), we have the minimax-problem $I_2(z_s^\star, s^\star) =$

$$\max_{0 \leq z_s \leq l} (\min_{s \in C}(\sigma_{min}(O_2) - n\sigma_{max}(O_2)\epsilon)) \qquad (22)$$

For this optimization problem, the outer maximization will be done by simply calculating $I_2(z_s, s^\star)$ over the full range $0 \leq z_s \leq l$. This gives also an overview for the distribution of the observability in the whole range.

A more difficult task is the minimization step in I_2 (nonconvex problem). As mentioned in section 4, a possible solution is to replace it by a lower bound, for which an algorithm was derived in [2]. This algorithm leads to the criterion $I_4(z_s^\star) =$

$$\max_{0 \leq z_s \leq l} [k(\sigma_{min}(O_4) - n\sigma_{max}(O_4)\epsilon)] \qquad (23)$$

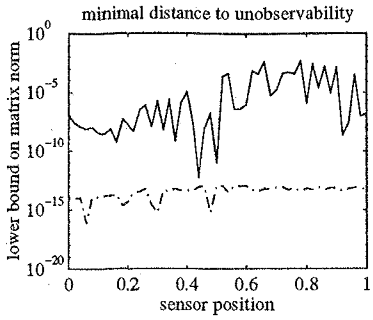

igure 4: observability measure $I_{r,4}(z_s)$ for a
20% uncertainty on k_0 and D_a

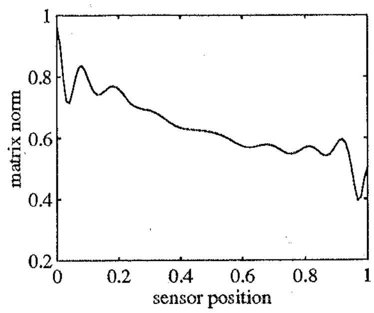

igure 5: Matrix 2-norm of $[\hat{A} - K\hat{C}]^{-1}\tilde{A}(\underline{p})$

here the matrix O_4 and the scalar k depend on ie pair (A, C). For the tubular reactor, $I_4(z_s)$ is iown in Figure 2c as the difference between the raight line and the dashed-dotted line.

If we have to deal with structured parameter ıcertainties, where the parameter vector $\underline{p}$ is ıown to be in the range $\underline{p}_l \leq \underline{p} \leq \underline{p}_u$, the crite- on I_4 can be extended to a "worst case"-design. herefore we treat the pair (A, C) as functions of In this case I_4 is extended to $I_{r,4}(z_s^\star, \underline{p}^\star) =$

$$\max_{0 \leq z_s \leq l} \left\{ \min_{\underline{p}_l \leq \underline{p} \leq \underline{p}_u} \{I_{r,4}(z_s, \underline{p})\} \right\} \tag{24}$$

ith $I_{r,4}(z_s, \underline{p}) = k(z_s, \underline{p})(\sigma_{min}(O_4(z_s, \underline{p}))$ - $n\ \sigma_{max}$ $O_4(z_s, \underline{p}))\ \epsilon)$ In figure 4, $I_{r,4}$ is shown for the tubu- ır reactor example, for a $\pm 20\%$ uncertainty on k_0 nd D_a. From figure 4 it can be seen that the ob- ɛrvability measure is reduced, but the system is ill observable over the whole interval $0 \leq z_s \leq l$. o get more insight into the effect of parameter ncertainties on state observation, let us look at ıeir influence on the state error dynamics and on ıe steady state error. When the observer:

$$\dot{\hat{\underline{x}}} = \hat{A}\hat{\underline{x}} + \hat{B}\underline{u} + K(\underline{y} - \hat{\underline{y}}), \qquad \hat{\underline{y}} = \hat{C}\hat{\underline{x}} \tag{25}$$

applied to the model (7) the state error dynam- s in the Laplace transform are equal to :

$$\tilde{\underline{X}}(s) = [sI - \hat{A} + K\hat{C}]^{-1}\{[\tilde{A} - K\tilde{C}]\underline{X}(s)$$

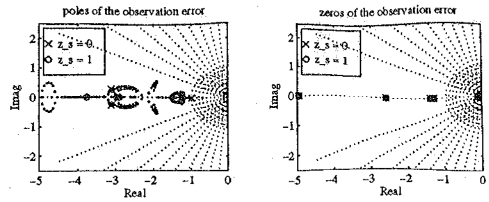

Figure 6: Poles and zeros of the output error transfer matrix

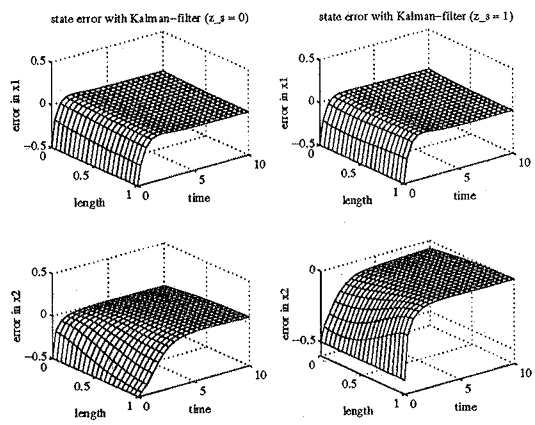

Figure 7: State error for $z_s = 0$ and $z_s = 1$ with faulty model

$$+\tilde{B}\underline{U}(s)\} \tag{26}$$

with $\tilde{\underline{X}} = \underline{X} - \hat{\underline{X}}$, $\tilde{A} = A - \hat{A}$, $\tilde{B} = B - \hat{B}$, $\tilde{C} = C - \hat{C}$. The dynamics of the output error $\tilde{\underline{y}} = \underline{y} - \hat{\underline{y}}$ is given in the Laplace transform by : $\tilde{\underline{Y}} = [I - \hat{C}[sI - \hat{A} + K\hat{C}]^{-1}K]\underline{Y}$ Let us consider here that only A is influenced by the parameter uncertainty. Then 26 is reduced to :

$$\tilde{\underline{X}} = [sI - \hat{A} + K\hat{C}]^{-1}\tilde{A}(\underline{p})\underline{X} \tag{27}$$

The steady state error is obtained from (27) $\tilde{\underline{x}} = -[\hat{A} - K\hat{C}]^{-1}\tilde{A}(\underline{p})\underline{x}$ and for the 2-norm of the steady state error, we have :

$$||\tilde{\underline{x}}||_2 \leq ||[\hat{A} - K\hat{C}]^{-1}\tilde{A}(\underline{p})||_2||\underline{x}||_2 \tag{28}$$

Thus, if we minimize $||[\hat{A} - K\hat{C}]^{-1}\tilde{A}(\underline{p})||_2$, which is a function of the sensor position and the uncertain parameters, we will reduce the sensitivity of the steady state error to these parameter uncertainties. So the optimal sensor position $z_s^\star$ can be found through the solution of $I_5(z_s^\star, \underline{p}^\star) =$

$$\min_{0 \leq z_s \leq l} \left\{ \max_{\underline{p}_l \leq \underline{p} \leq \underline{p}_u} \{||[\hat{A} - K\hat{C}]^{-1}\tilde{A}(\underline{p})||_2\} \right\} \tag{29}$$

For the above supposed uncertainties $I_5(z_s, \underline{p}^\star)$ is shown in Figure 5. For the matrix K a stationary

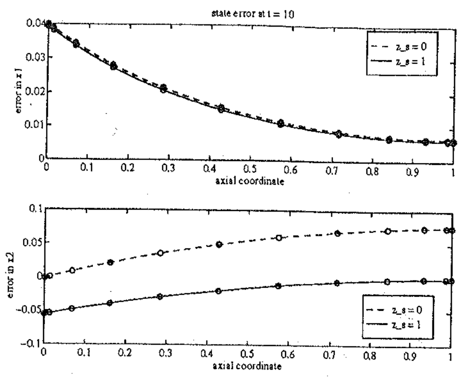

Figure 8: Steady state error for $z_s = 0$ and $z_s = 1$ with faulty model

Kalman filter was used. From Figure 5 the optimal sensor position $z_s^\star$ is close to 1.

To analyse the influence of the sensor position on the error dynamics, the pole and zero distribution of the transfer matrix from Y to the output error $\tilde{Y}$ is shown in Figure 6. Outside of the range of this figure we have only some poles and zeros near to the real axis on the negative half plane, which do not considerably move with a variation in z_s. Note, that the poles and zeros only depend on the observer matrices. From Figure 6 it can be seen that there is no important change in the error dynamics when z_s is moved from 0 to l.

In order to illustrate the influence of the sensor position on the state estimation, a deviation of 20% in the specific reaction rate k_0 and in the diffusion constant D_a is applied in the observer model. The state error $\tilde{\underline{x}}_1(z,t)$, $\tilde{\underline{x}}_2(z,t)$ and the resulting steady state error are shown for 2 sensor positions in figure 7 and figure 8. From these figures it can be seen that the sensor position obtained from (29) reduces the steady state error.

6 Conclusions

In this paper we have discussed the choice of sensor positions for a tubular reactor with a preset number of sensors. Different observability measures, based on the observability matrix, the observability gramian and the Popov-Belevitch-Hautus rank test have been considered. The analysis has been carried out on the reduced finite-dimensional model of the process. The results of these investigations were put in perspective with the modal observability properties of the original infinite-dimensional model. In particular it has been shown that the collocation method represents an approximation for the dominant low order eigenmodes of the distributed parameter model. In that sense we can conclude that when the computation of the system eigenmodes is too complex, the orthogonal collocation appears to be an interesting approximation for the (modal) observability analysis because of its ability to fairly approximate the loss of observability at the zeros of the dominant system eigenfunctions.

Acknowledgment This paper includes results of the Network in Chemical Process Control which is supported by the Human Capital and Mobility program of the European Community (Contract CHRX-CT94-0672). It presents research results of the Belgian Programme on Inter-University Poles of Attraction initiated by the Belgian State, Prime Minister's office for Science, Technology and Culture. The scientific responsibility rests with its authors.

References

[1] E. Anderson, Z. Bai, C. Bischof, J. Demmel, J. Dongarra, J. Du Croz, A. Greenbaum, S. Hammarling, A. McKenney, S. Ostrouchov, and D. Sorensen. *LAPACK User's Guide*. SIAM, Philadelphia, 1992.

[2] D. Boley. Estimating the sensitivity of the algebraic structure of pencils with simple eigenvalue estimates. *SIAM J. Mat. Anal. Appl.*, 11(4):632-643, 1990.

[3] F. M. Callier and C. A. Desoer. *Linear System Theory.* Springer-Verlag, New York, 1991.

[4] R. F. Curtain and H. J. Zwart. *An Introduction to Infinite-Dimensional Linear Systems Theory.* Springer-Verlag, Berlin, 1995.

[5] D. Dochain and J. Winkin. Dynamical analysis of a class of distributed parameter fixed bed reactors. *Proc. CDC'95*, 3225-3230, 1995.

[6] R. Eising. Between controllable and uncontrollable. *Syst. Cont. Lett.*, 4:263-264, 1984.

[7] C. Georgakis, R. Aris, and R. Amundson. Studies in the control of tubular reactors - I. General considerations. *Chem. Eng. Sci.*, 32:1359-1369, 1977.

[8] T.J. Harris, J. F. MacGregor, and J. D. Wright. Optimal sensor location with an application to a packed bed tubular reactor. *AICHE J.l*, 26(6):910-916, 1980.

[9] T. Kailath. *Linear Systems.* Prentice-Hall, Englewood Cliffs, 1980.

[10] The Mathworks Inc., Natick. *Matlab Ref. Man., Version 4.2a*, 1994.

[11] W. Waldraff and D. Dochain. On the use of observability measures for sensor location in fixed bed reactors. *Cesame, UCL, Int. Rep. 96-09*, 1996.